Supporting Information

Cucurbit[*n*]urils-based host-guest interaction enhancing organic room-temperature phosphorescence of phtalic anhydride derivatives in aqueous solution

Tianyue Xu,[a] Fengbo Liu,[a] Xianchen Hu,[a] Zhiyong Zhao,[a,b] Simin Liu[*a,b]

[a] School of Chemistry and Chemical Engineering, Wuhan University of Science and Technology, Wuhan 430081, China. E-mail: liusimin@wust.edu.cn

[b] The State Key Laboratory of Refractories and Metallurgy, Institute of Advanced Materials and Nanotechnology, Wuhan University of Science and Technology, Wuhan 430081, China.

Table of Contents

General Experimental Section.

CB[8] and CB[10] were prepared by the corresponding literature procedures.[1,2] Other compounds used in this study were purchased from commercial suppliers and were used without further purification. NMR spectra (^{1}H, ^{13}C) were collected on Agilent 600 MHz DD2 spectrometers. Mass spectrometry was performed using a Bruker FT-ICR Apex IV qQ equipped 12T super conducting magnet. UV/Vis were performed on a SHIMADZU UV-3600 instrument with 1 cm pathlength cells at 298 K. ITC data was measured using TA NANO ITC instrument. Photoluminescence spectra were measured on a PerkinElmer LS-55 machine. Phosphorescence lifetime was recorded using a FS5 instrument (Edinburg instruments, Livingstone, UK). A Suprasil Quartz (QS) cuvette with 1 cm path length was used for all measurements. The data was fitted with the exponential reconvolution function and the non-linear least square method.

Synthesis and characterization

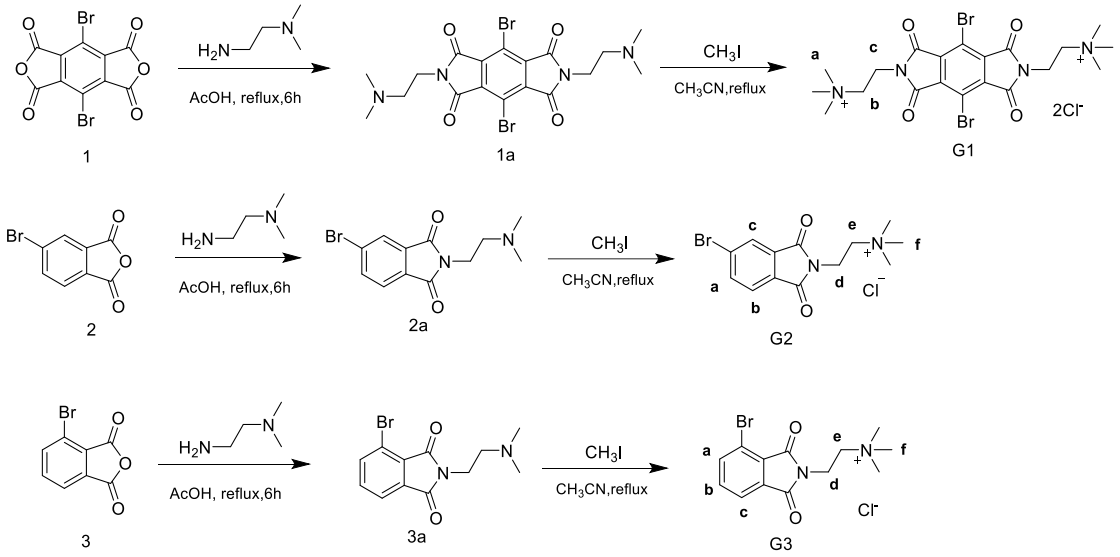

Scheme S1. Synthesis route of phtalic anhydride derivates **G1-G3**.

Synthesis of **G1-G3** were modified from previously reported procedures.[3,4]

4,8-dibromo-2,6-bis(2-(dimethylamino)ethyl)pyrrolo[3,4-f]isoindole-1,3,5,7(2H,6H)-tetraone (**1a**)
Compound **1** (0.187 g, 0.5 mmol) and 2-dimethylaminoethylamine (0.176 g, 2 mmol) were added in acetic acid (30 ml), the mixture was refluxed for 6 h in oil bath. The resultant solution was extracted with dichloromethane, and then organic phase was evaporated under reduced pressure and then purified by silicagel column chromatography(dichloromethane/methanol=50:1) to afford **1a** (73 mg, 28%) as pink solid. ^{1}H NMR (600 MHz, $CDCl_3$) δ (ppm): 3.84 (t, *J* = 6.0 Hz, 2H), 2.60 (t, *J* = 6.6 Hz, 2H), 2.26 (s, 6H).

5-bromo-2-(2-(dimethylamino)ethyl)isoindoline-1,3-dione (**2a**)
Compound **2** (0.226 g, 1 mmol) and 2-dimethylaminoethylamine (0.176 g, 2 mmol) were added in acetic acid (30 ml), the mixture was refluxed for 6 h in oil bath. The resultant solution was extracted with dichloromethane, and then organic phase was evaporated under reduced pressure and then purified by silicagel column chromatography (dichloromethane/methanol=50:1) to afford **2a** (172 mg, 58%) as yellow solid. ^{1}H NMR (600 MHz, DMSO-d_6) δ (ppm): 8.04 (s, 1H), 8.01 (d, *J* = 7.8 Hz, 1H), 7.78 (d, *J* = 8.4 Hz, 1H), 3.64 (t, *J* = 6.6 Hz, 2H), 2.44 (t, *J* = 6.6 Hz, 2H), 2.12 (s, 6H).

4-bromo-2-(2-(dimethylamino)ethyl)isoindoline-1,3-dione (**3a**)
Compound **3** (0.226 g, 1 mmol) and 2-dimethylaminoethylamine (0.176 g, 2 mmol) were added in acetic acid (40 ml), the mixture was refluxed for 6 h in oil bath. The resultant solution was extracted with dichloromethane, and the organic phase was evaporated under reduced pressure and then purified by silicagel column chromatography (dichloromethane/methanol=50:1) to afford **3a**

(146 mg, 49%) as white solid. ^{1}H NMR (600 MHz, $CDCl_3$) δ (ppm): 7.98 (d, *J* = 2.4 Hz, 1H), 7.85 (d, *J* = 7.8 Hz, 1H), 7.71 (d, *J* = 8.4 Hz, 1H), 4.01 (t, *J* = 7.8 Hz, 2H), 3.15 (t, *J* = 6.6 Hz, 2H), 2.71 (s, 6H).

2,2'-(4,8-dibromo-1,3,5,7-tetraoxo-5,7-dihydropyrrolo[3,4-f]isoindole-2,6(1H,3H)-diyl)bis(N,N,N-trimethylethan-1-aminium) (**G1**)

To a solution of DCM (30 ml) was added compound **1a** (51 mg, 0.1 mmol), methyl iodide (1 ml) was then added, the mixture was refluxed for 24 h in oil bath. The resultant solution was cooled to room temperature and evaporated under reduced pressure, the residue was washed by DCM for three times and dried at 60 ℃ in vacuum. The solid was dissolved in H_2O, added KPF_6 and the precipitate was centrifuged, washed by H_2O for three times. The solid was dissolved in CH_3CN and $Bu_4N^+Cl^-$ was added, the precipitate was washed by CH_3CN for three times to afford **G1** (31 mg, 51%) as pink-white solid. ^{1}H NMR (600 MHz, D_2O) δ (ppm): 4.12 (t, *J* = 7.2 Hz, 2H), 3.56 (t, *J* = 6.6 Hz, 2H), 3.14 (s, 9H). ^{13}C NMR (151 MHz, D_2O) δ (ppm): 164.4, 136.3, 109.9, 62.0, 53.3, 32.2. HRMS (ESI): *m/z* $[M\text{-}2Cl^-]^{2+}$ calcd. for $C_{20}H_{26}Br_2N_4O_4^{2+}$: 272.0159, found: 272.0154.

Products **G2** and **G3** were synthesized via the same procedures as **G1**.

2-(5-bromo-1,3-dioxoisoindolin-2-yl)-N,N,N-trimethylethan-1-aminium chloride (**G2**)

Faint yellow solid (89 mg, 63%). ^{1}H NMR (600 MHz, D_2O) δ (ppm): 7.97 (s, 1H), 7.91 (d, *J* = 7.8 Hz, 1H), 7.68 (d, *J* = 8.4 Hz, 1H), 4.05 (t, *J* = 7.2 Hz, 2H), 3.54 (t, *J* = 6.6 Hz, 2H), 3.11 (s, 9H). ^{13}C NMR (151 MHz, D_2O) δ (ppm): 168.8, 168.2, 137.8, 132.9, 129.9, 129.1, 126.8, 125.0, 62.4, 53.2, 31.8. HRMS (ESI): *m/z* $[M\text{-}2Cl^-]^{1+}$ calcd. for $C_{13}H_{16}BrN_2O_2^{1+}$: 311.0389, found: 311.0389.

2-(4-bromo-1,3-dioxoisoindolin-2-yl)-N,N,N-trimethylethan-1-aminium chloride (**G3**)

White solid (92 mg, 65%). ^{1}H NMR (600 MHz, D_2O) δ (ppm): 7.84 (d, *J* = 8.4 Hz, 1H), 7.75 (d, *J* = 7.8 Hz, 1H), 7.57 (t, *J* = 7.8 Hz, 1H), 4.07 (t, *J* = 6.6 Hz, 2H), 3.56 (t, *J* = 7.2 Hz, 2H), 3.13 (s, 9H). ^{13}C NMR (151 MHz, D_2O) δ (ppm): 167.9, 167.6, 139.4, 135.9, 133.4, 128.9, 122.9, 118.1, 62.4, 53.3, 31.8. HRMS (ESI): *m/z* $[M\text{-}2Cl^-]^{1+}$ calcd. for $C_{13}H_{16}BrN_2O_2^{1+}$: 311.0389, found: 311.0389.

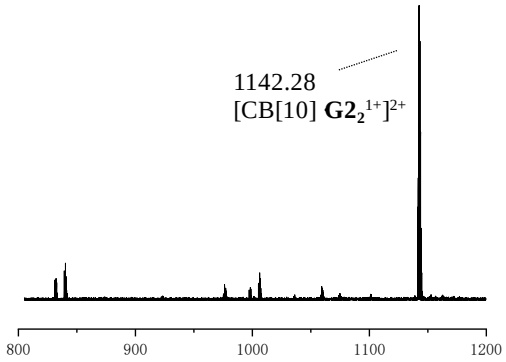

Figure S1. ESI-MS spectral of compound **G2** with 1 equiv. of CB[10]. The ion at m/z = 1142.28 which corresponds to the 1:2 complex CB[10] 2**G2** ([CB[10] + 2**G2**$^{1+}$]$^{2+}$ = 1142.29) was observed.

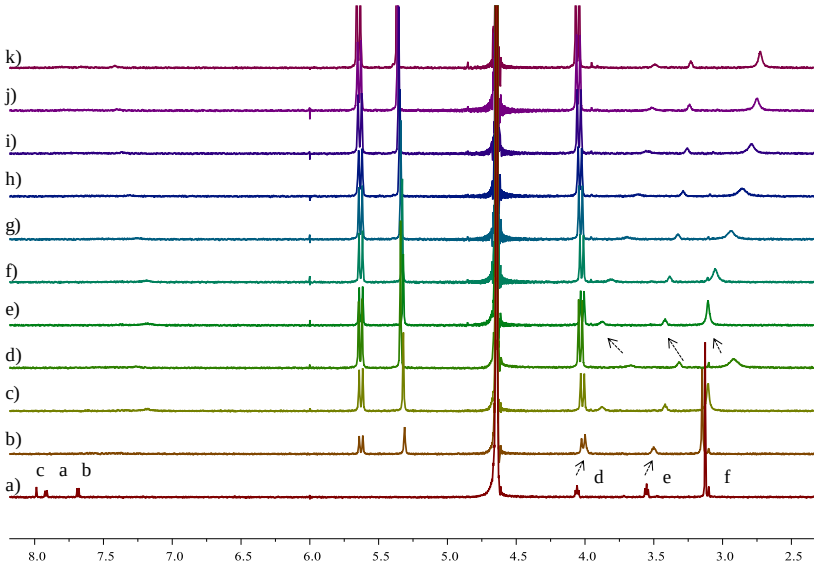

Figure S2. ^{1}H NMR spectra recorded(600 MHz, D_2O, 298K) for compound **G2** (1.0 mM) with addition of different equivalences of CB[8]: (a) 0, (b) 0.1, (c) 0.2, (d) 0.3, (e) 0.4, (f) 0.5, (g) 0.6, (h) 0.7, (i) 0.8, (j) 0.9, (k) 1.0.

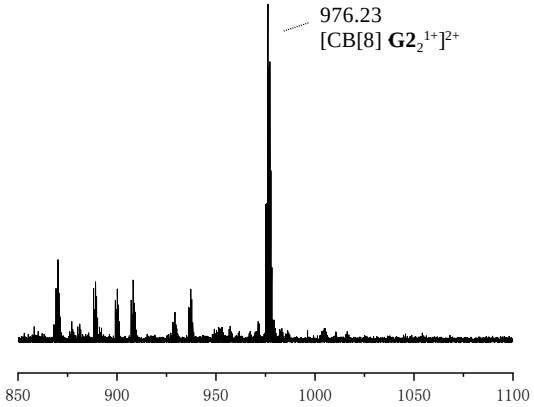

Figure S3. ESI-MS spectral of compound **G2** with 1 equiv. of CB[8]. The ion at m/z = 976.23 which corresponds to the 1:2 complex CB[8] 2**G2** ([CB[8] + 2**G2**$^{1+}$]$^{2+}$ = 976.23) was observed.

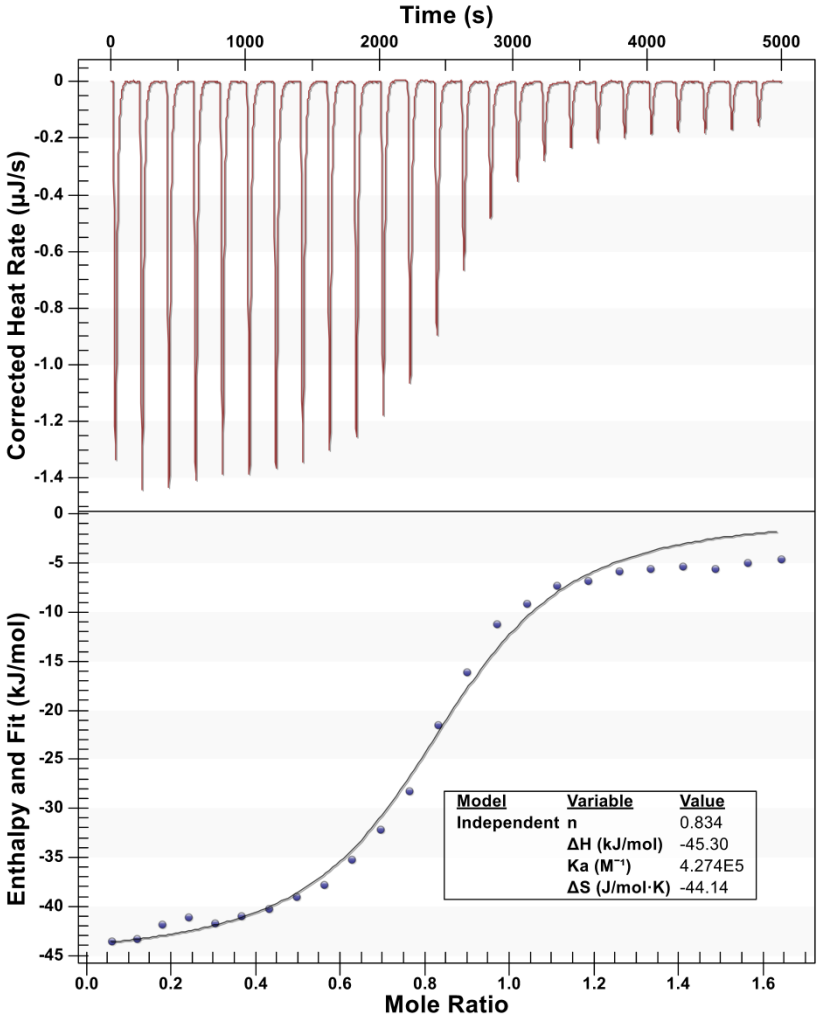

Figure S4. The ITC data for **G2** with CB[8] in water.

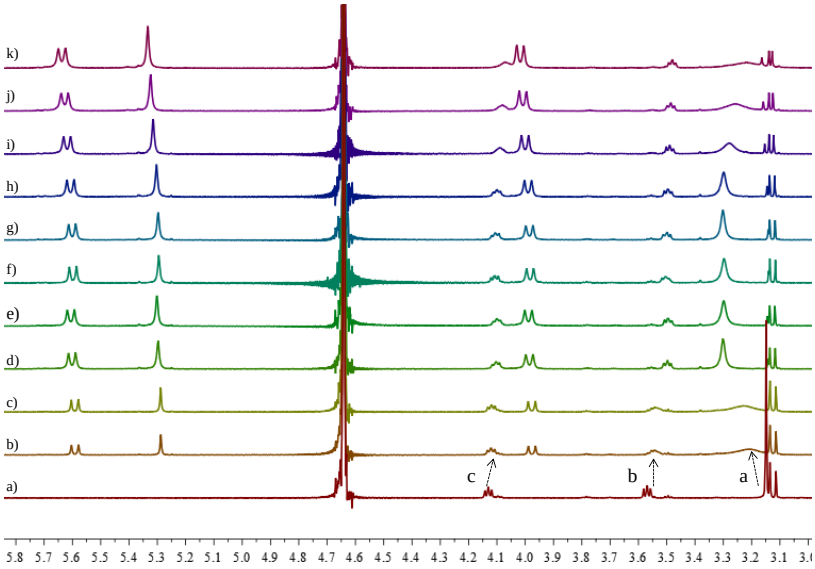

Figure S5. ^{1}H NMR spectra recorded(600 MHz, D_2O, 298K) for compound **G1** (1.0 mM) upon titration of different amounts of CB[10]: (a) 0, (b) 0.1, (c) 0.2, (d) 0.3, (e) 0.4, (f) 0.5, (g) 0.6, (h) 0.7, (i) 0.8, (j) 0.9, (k) 1.0 equiv.

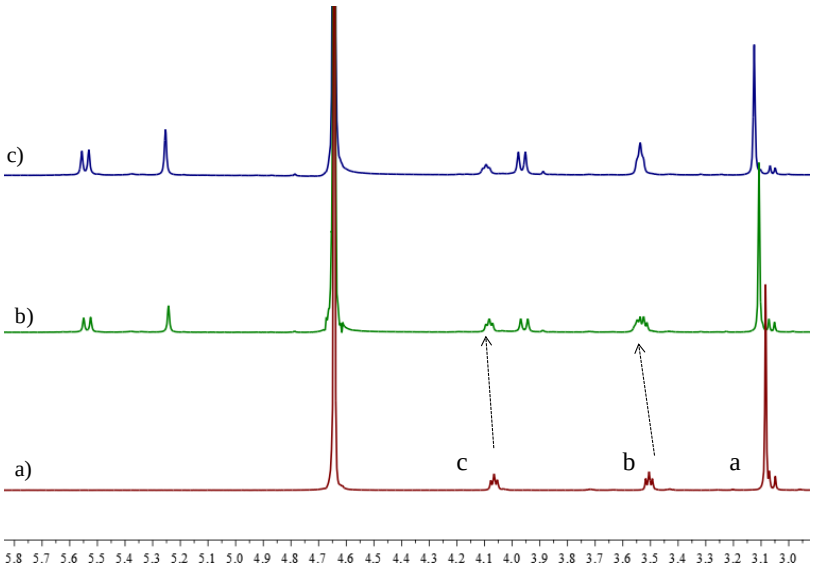

Figure S6. ^{1}H NMR spectra recorded (600 MHz, D_2O, 298K) for compound **G1** (1.0 mM) with addition of different equivalences of CB[8] (a) 0, (b) 0.5, (c) 1.0.

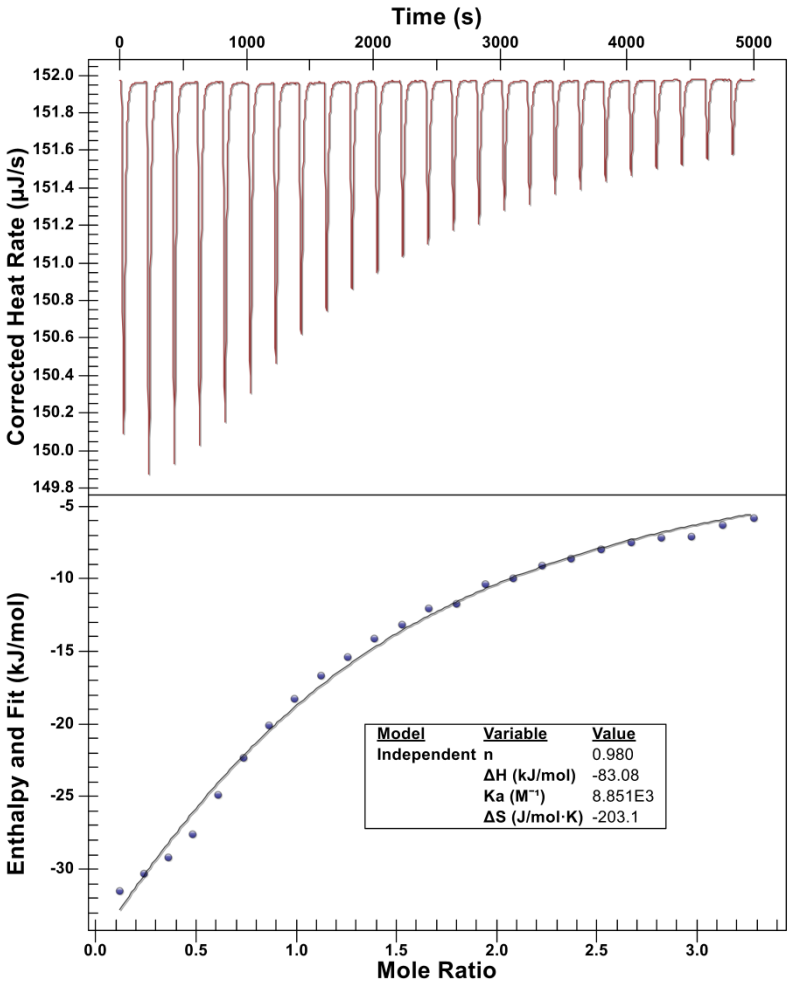

Figure S7. The ITC data of **G1** with CB[8] in water.

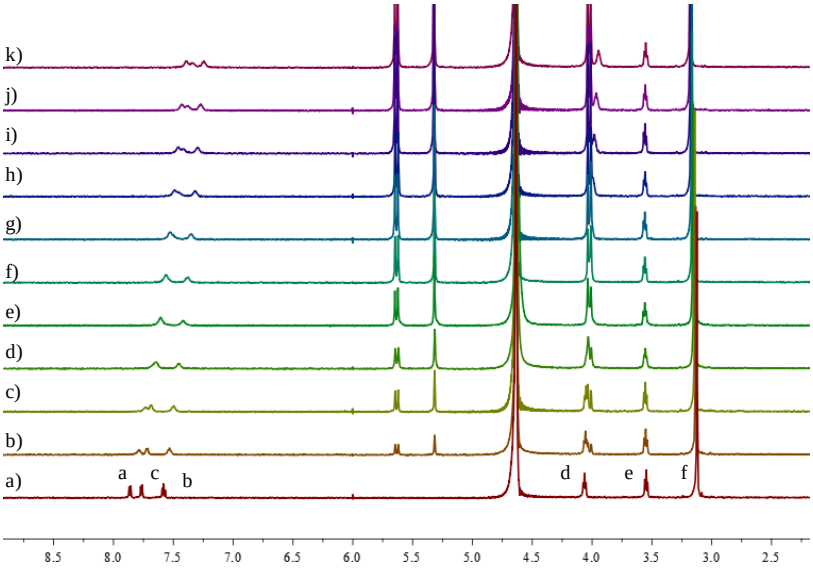

Figure S8. ^{1}H NMR spectra recorded (600 MHz, D_2O, 298K) for compound **G3** (1.0 mM) with addition of different equivalences of CB[8]: (a) 0, (b) 0.1, (c) 0.2, (d) 0.3, (e) 0.4, (f) 0.5, (g) 0.6, (h) 0.7, (i) 0.8, (j) 0.9, (k) 1.0.

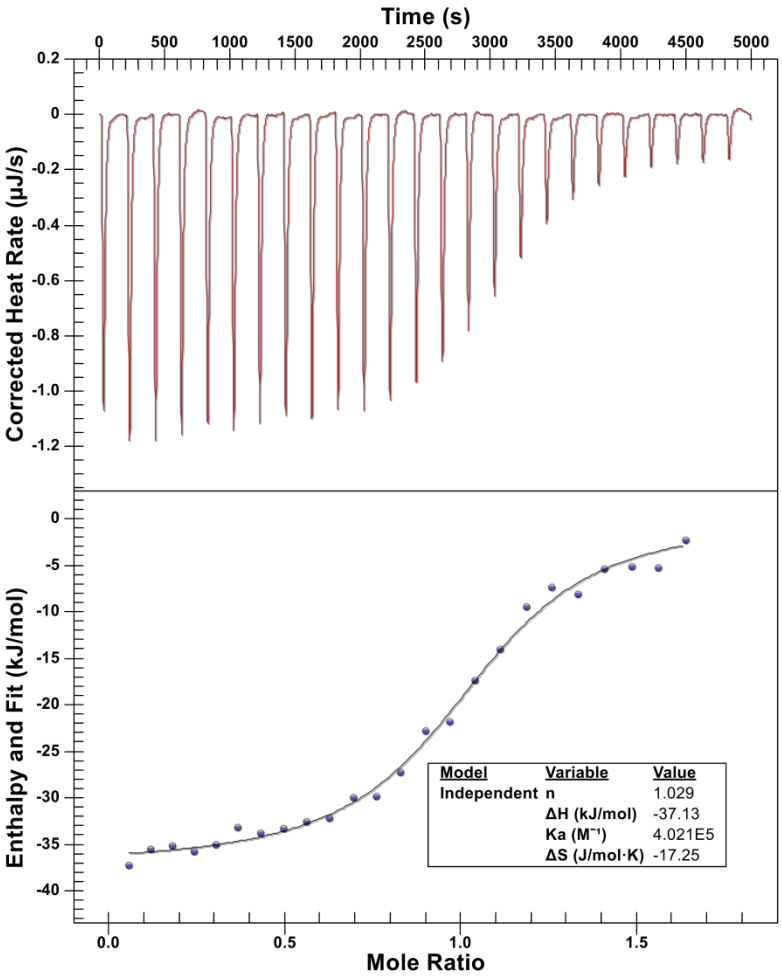

Figure S9. The ITC data of **G3** with CB[8] in water.

Table S1. Binding constants of **G1-G3** with CB[8].

Guest	Host	Binding constant (M^{-1})
G1	CB[8]	8.85×10^3
G2	CB[8]	4.27×10^5
G3	CB[8]	4.02×10^5

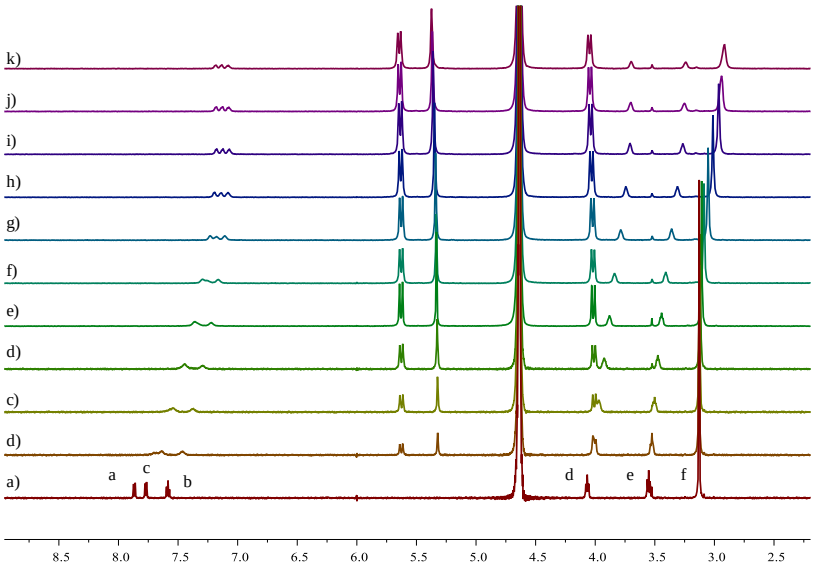

Figure S10. ^{1}H NMR spectra recorded(600 MHz, D_2O, 298K) for compound **G3** (1.0 mM) with addition of different equivalences of CB[10]: (a) 0, (b) 0.1, (c) 0.2, (d) 0.3, (e) 0.4, (f) 0.5, (g) 0.6, (h) 0.7, (i) 0.8, (j) 0.9, (k) 1.0.

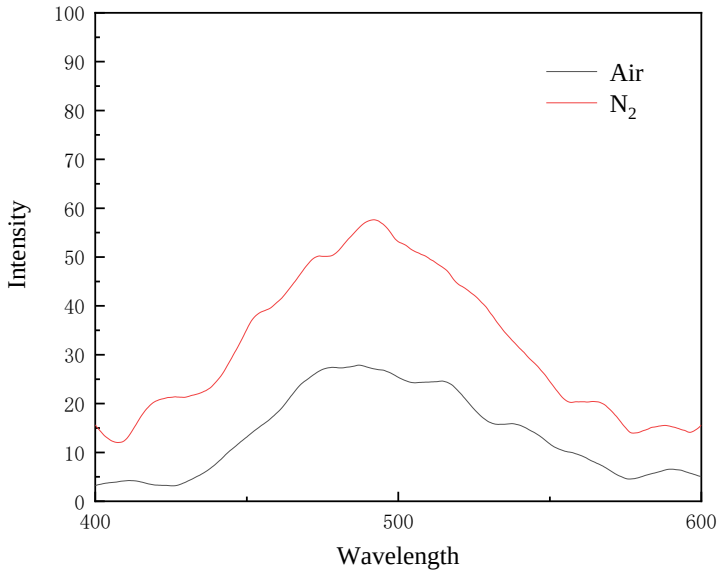

Figure S11. Phosphorescence spectra (delayed by 10 μs, slit width: e_x = 10 nm, e_m = 5 nm) of **G1** under air and N_2 atmosphere.

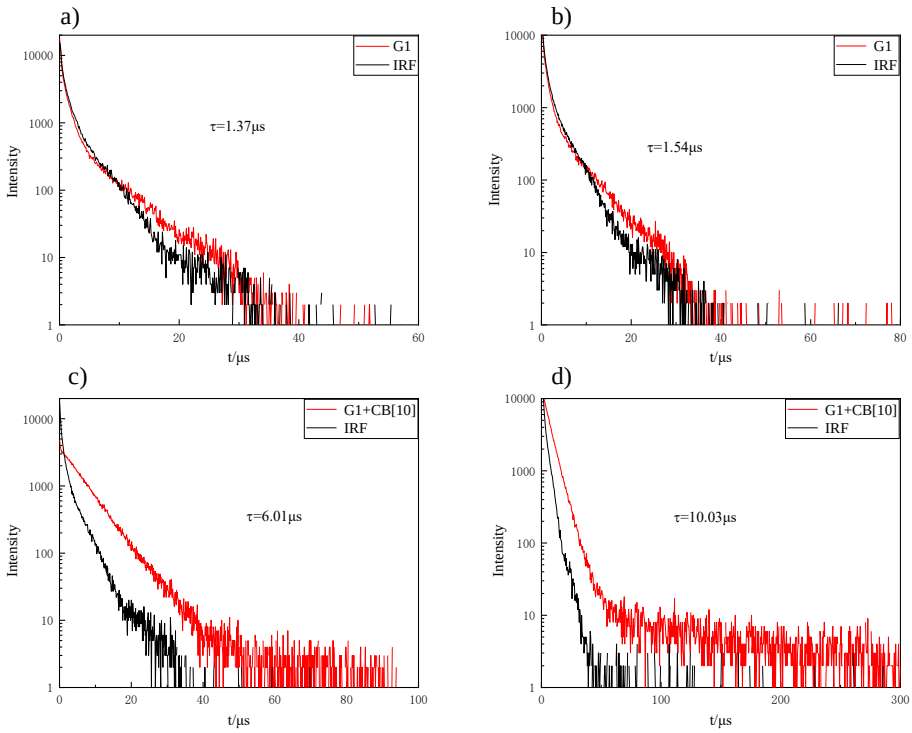

Figure S12. Phosphorescence lifetime decay curves of **G1** (a) under ambient condition; (b) under N_2 atmosphere and of **G1** with CB[10] (c) under ambient condition; (d) under N_2 atmosphere.

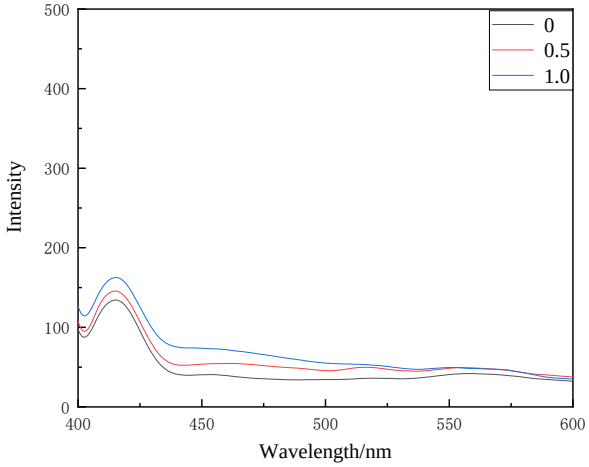

Figure S13. Photoluminescence spectra of **G1** (50μM) with addition of different equiv. of CB[8] in water (λ_{ex} = 340 nm; slit width: e_x= 10 nm, e_m = 5 nm).

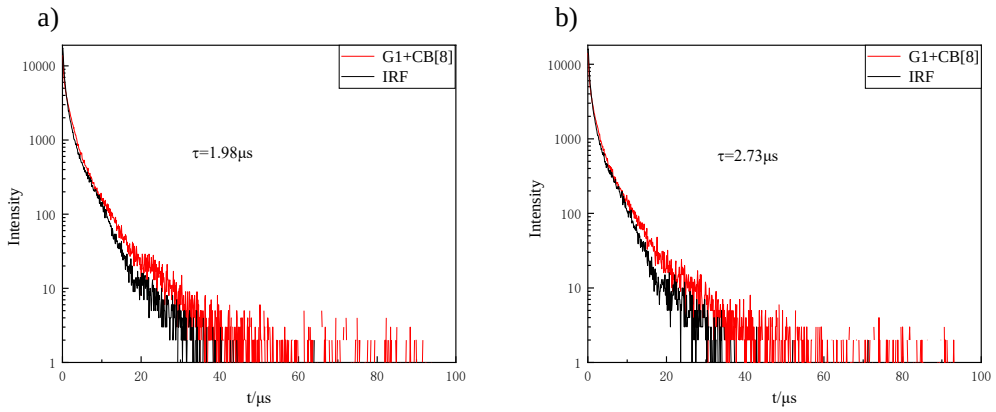

Figure S14. Phosphorescence lifetime decay curves of **G1** with CB[8] (a) under ambient condition ; (b) under N_2 atmosphere.

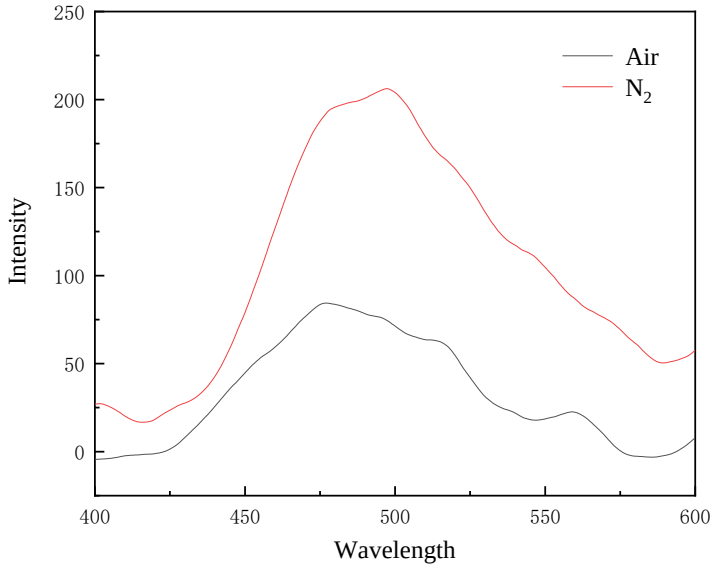

Figure S15. Phosphorescence spectra (delayed by 20 μs, slit width: e_x = 10 nm, e_m = 5 nm) of **G2** under air and N_2 atmosphere.

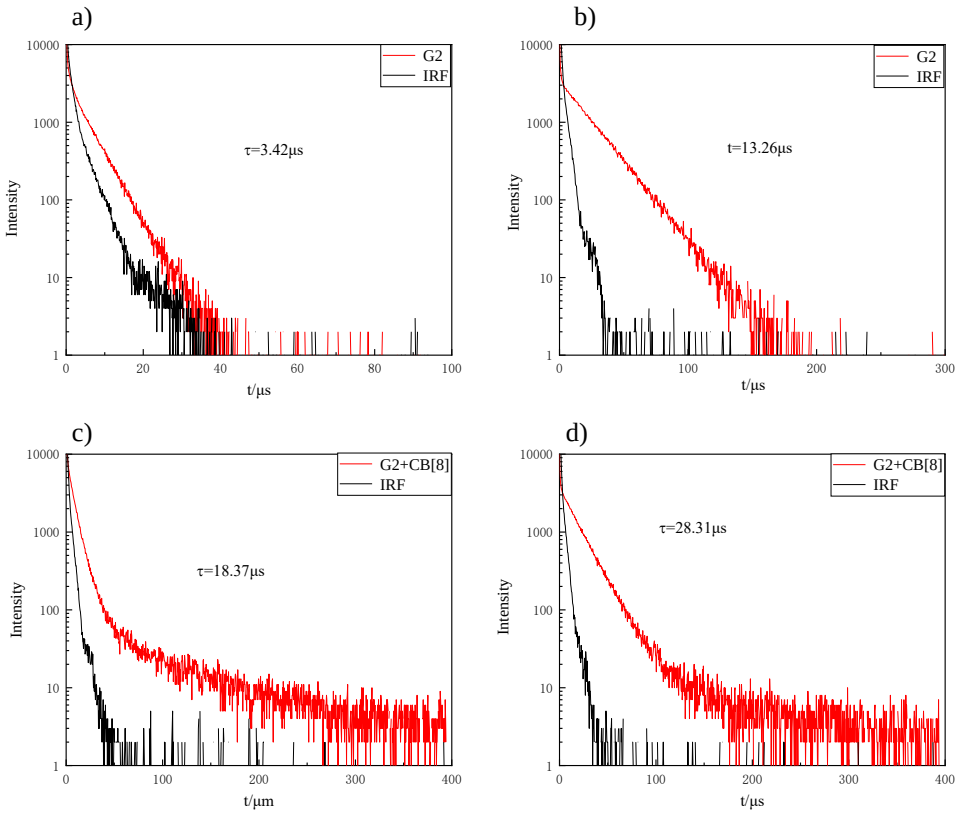

Figure S16. Phosphorescence lifetime decay curves of **G2** (a) under ambient condition; (b) under N_2 atmosphere and of CB[8] **G2** complex (c) under ambient condition; (d) under N_2 atmosphere.

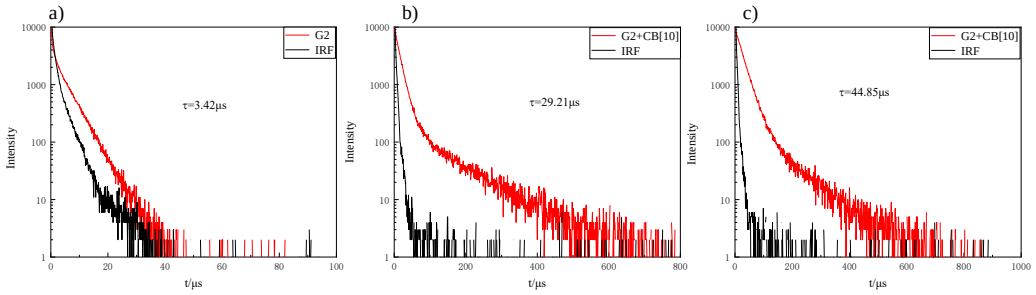

Figure S17. Phosphorescence lifetime decay curves of **G2** (a) under ambient condition and of CB[10] **G2** complex (b) under ambient condition; (c) under N_2 atmosphere.

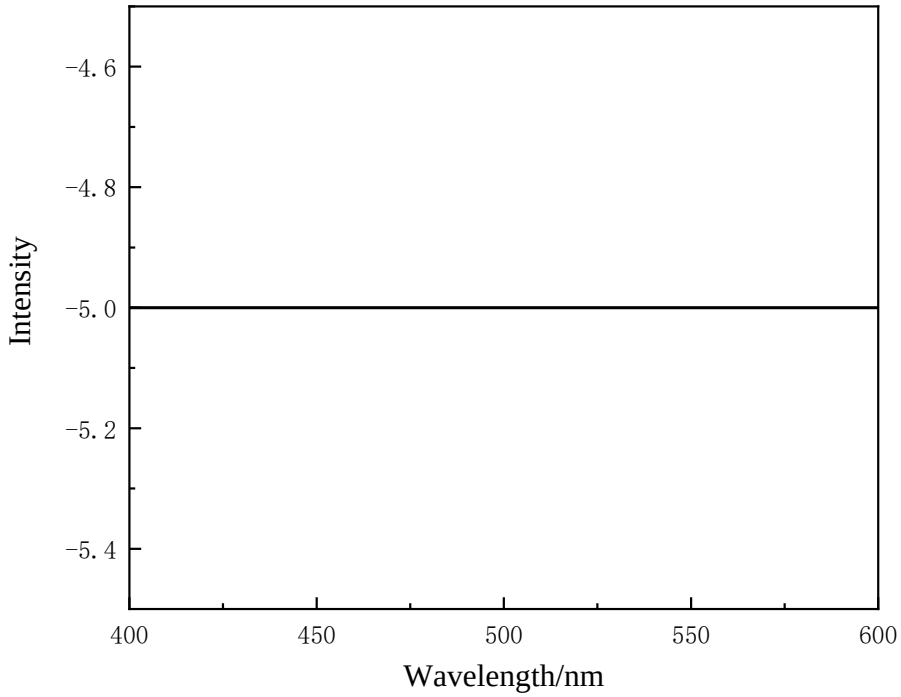

Figure S18. Phosphorescence spectra (delayed by 30 μs, slit width: e_x = 10 nm, e_m = 5 nm) of **G3** under air and N_2 atmosphere.

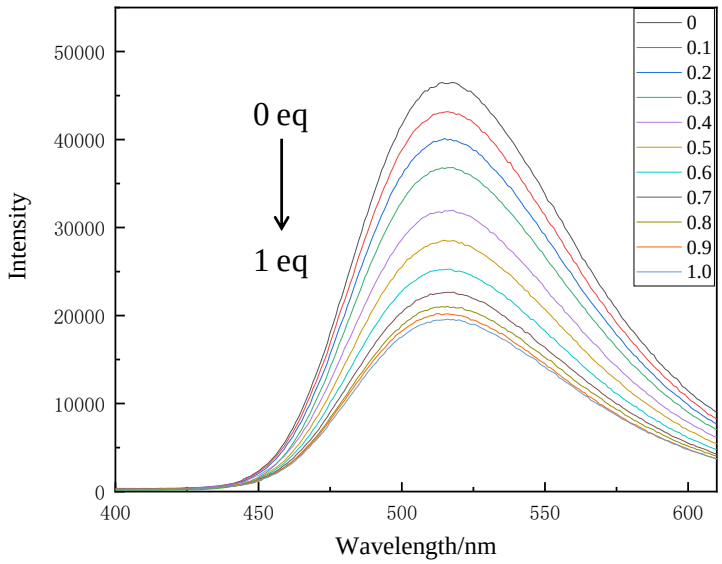

Figure S19. Photoluminescence spectra (λ_{ex}= 319 nm; slit width: e_x = 10 nm, e_m = 5 nm) of **G3** (50 μM) with different equivalences of CB[8] (0 - 1.0 equiv) in water.

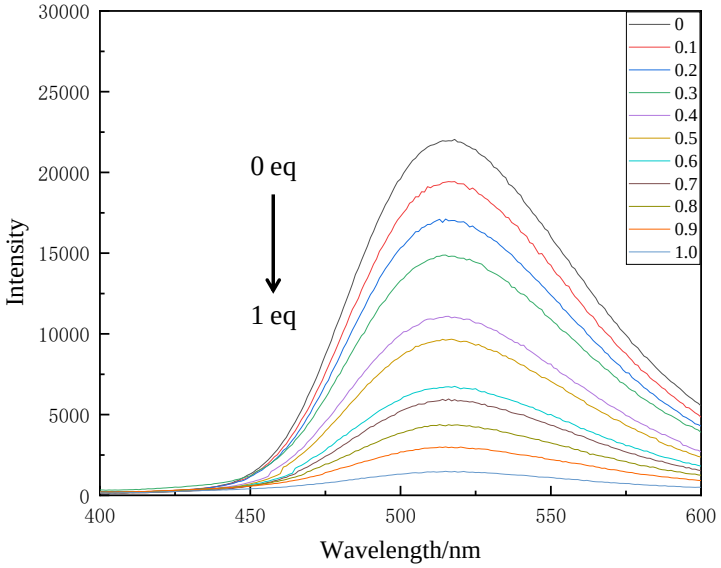

Figure S20. Photoluminescence spectra (λ_{ex}= 319 nm; slit width: e_x = 10 nm, e_m = 5 nm) of **G3** (50 μM) with different ratios of CB[10] (0 - 1.0 equiv) in water.

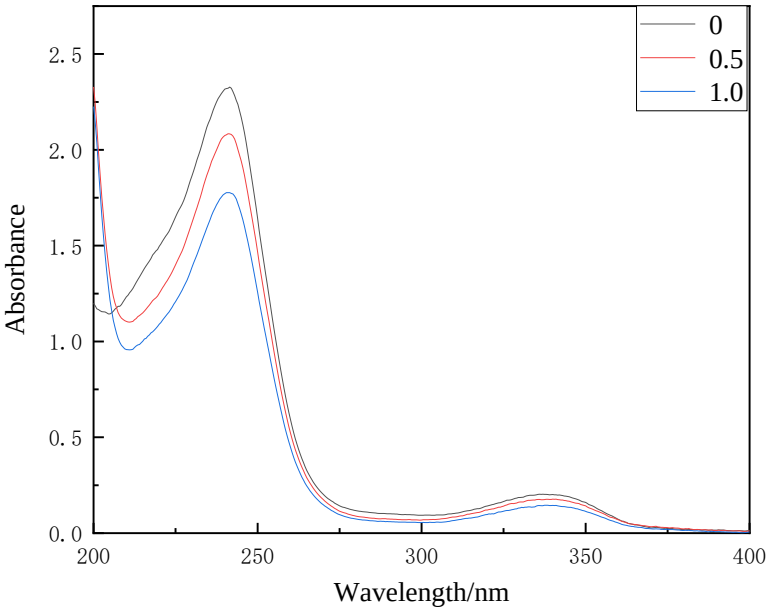

Figure S21. UV-Vis absorption spectra of **G1** (50 μM) with addition of different equiv. of CB[8].

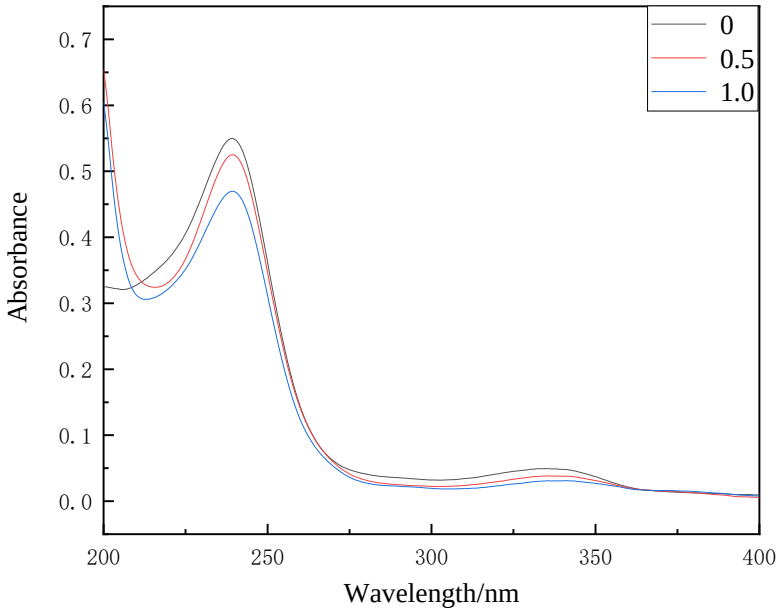

Figure S22. UV-Vis absorption spectra of **G1** (50 μM) with addition of different equiv. of CB[10].

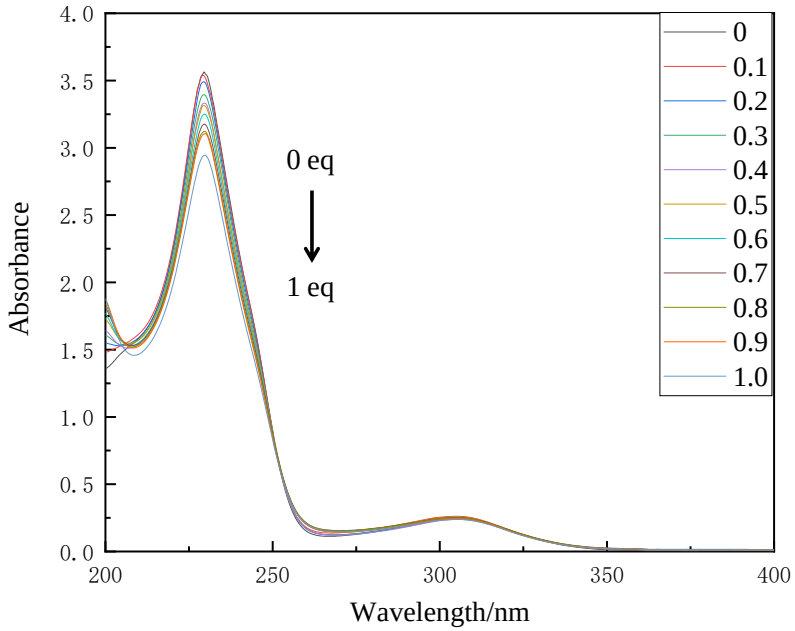

Figure S23. UV-Vis absorption spectra of **G2** (50 μM) with addition of different equiv. of CB[8].

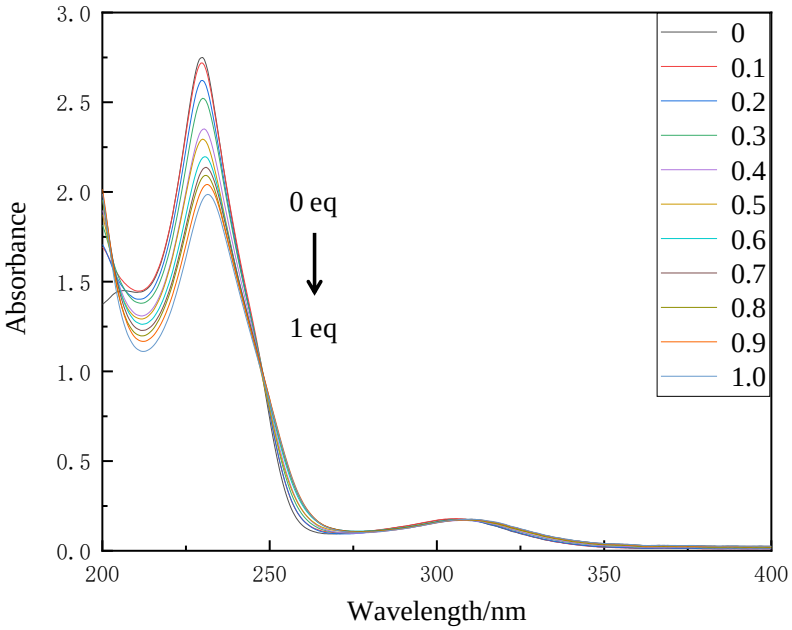

Figure S24. UV-Vis absorption spectra of **G2** (50 μM) with addition of different equiv. of CB[10].

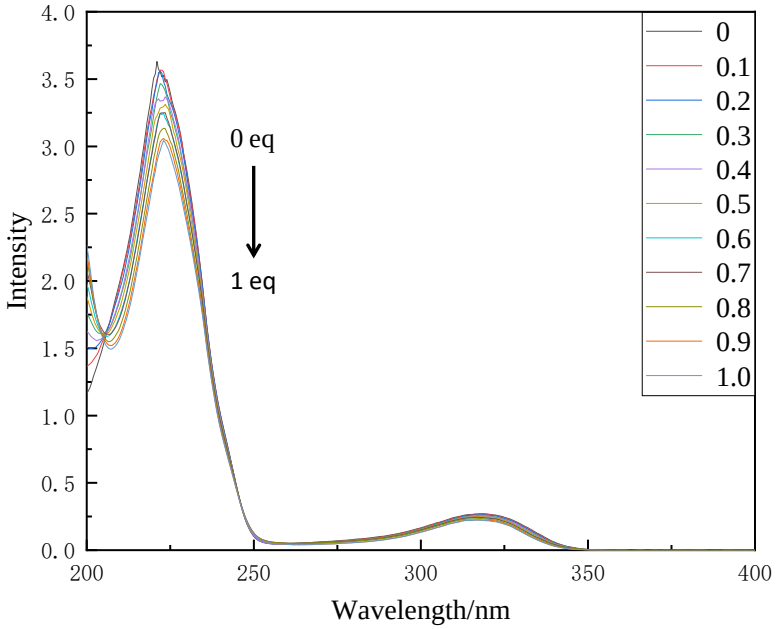

Figure S25. UV-Vis absorption spectra of **G3** (50 μM) with addition of different equiv. of CB[8].

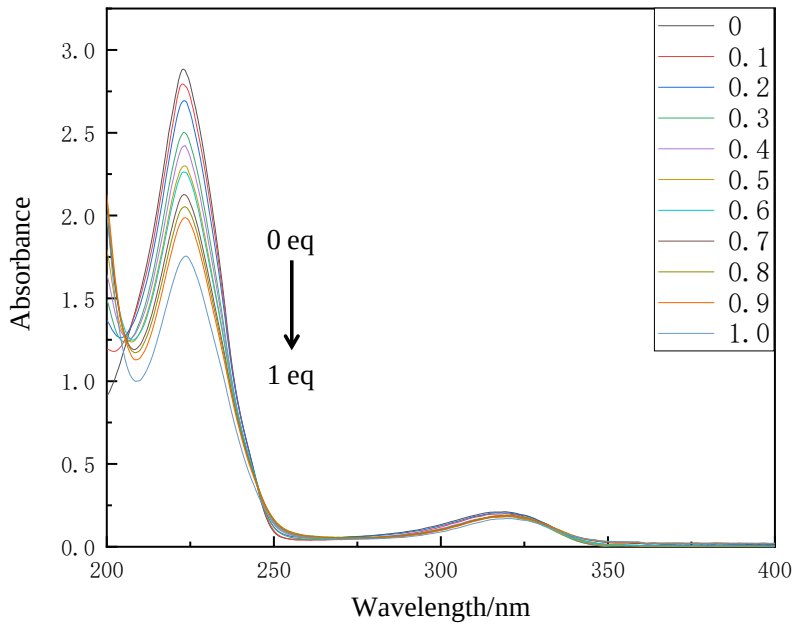

Figure S26. UV-Vis absorption spectra of **G3** (50 μM) with addition of different equiv. of CB[10].

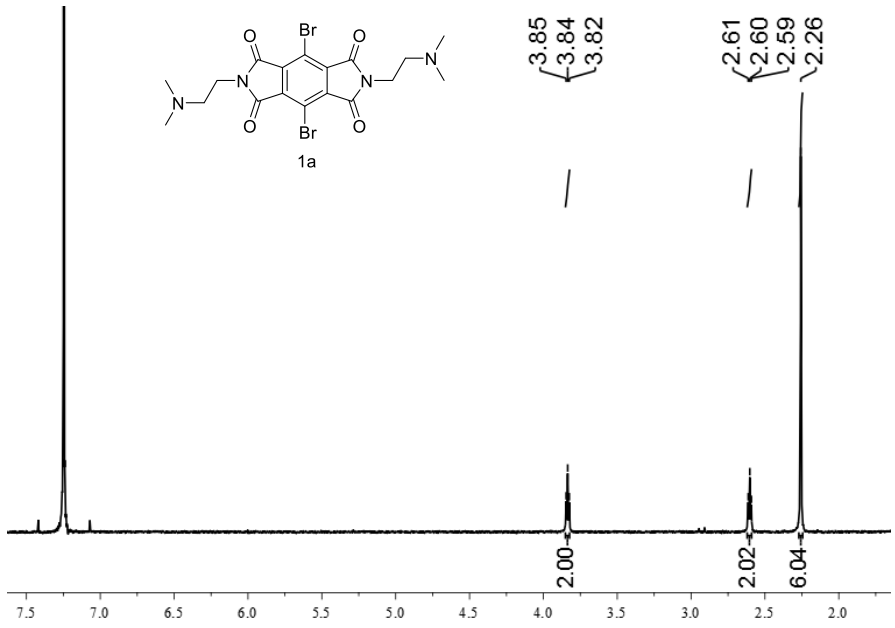

Figure S27. ^{1}H NMR spectra recorded (600 MHz, $CDCl_3$, 298K) for compound **1a** (1.0 mM) .

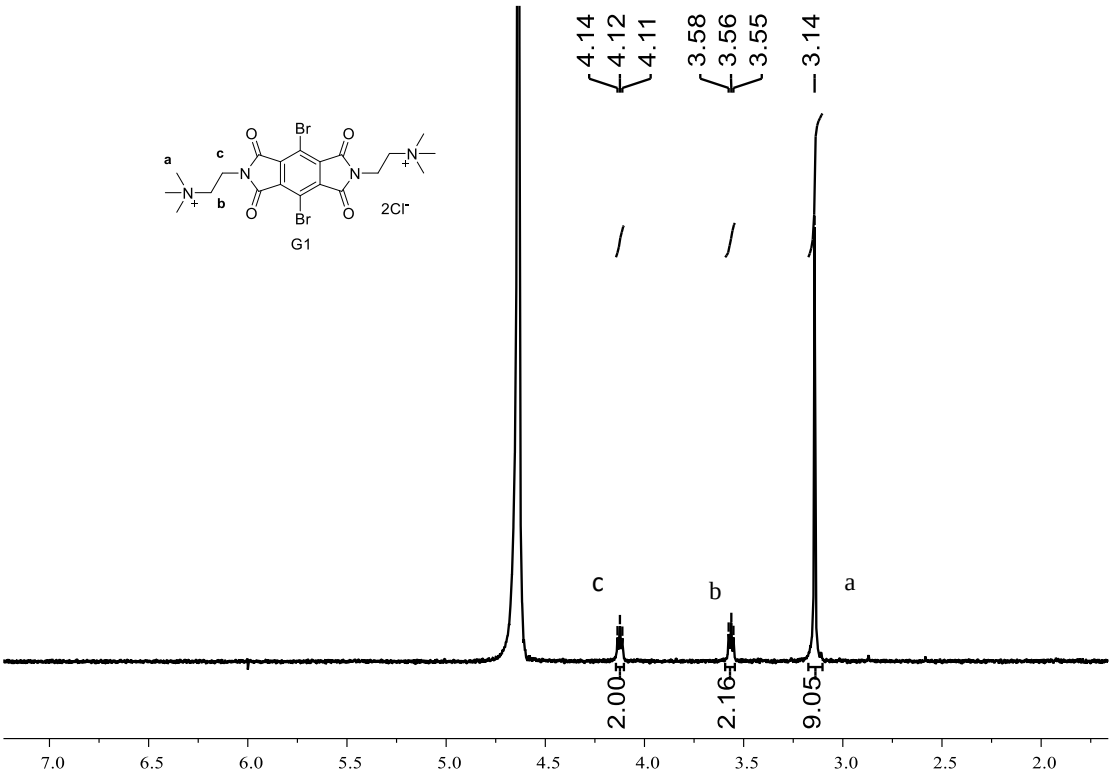

Figure S28. ^{1}H NMR spectra recorded (600 MHz, D_2O, 298K) for compound **G1** (1.0 mM) .

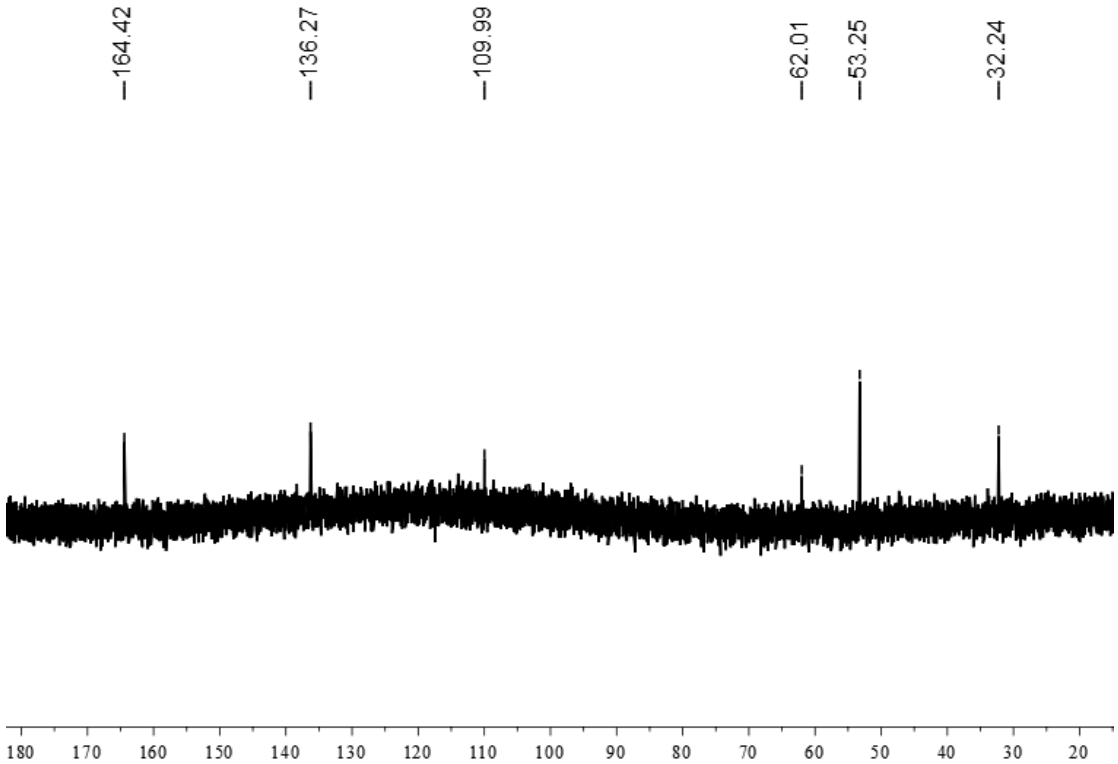

Figure S29. ^{13}C NMR spectra recorded (600 MHz, D_2O, 298K) for compound **G1** .

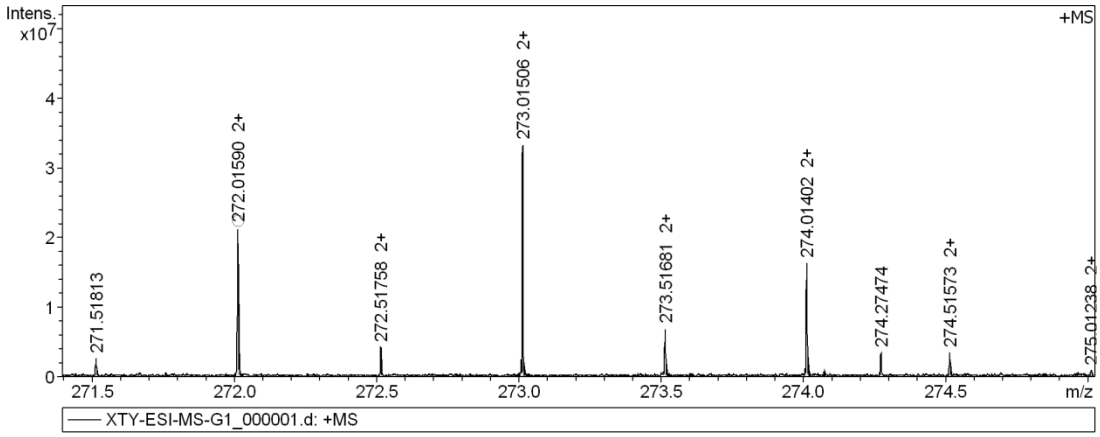

Figure S30. HRMS (ESI) spectrum of **G1**.

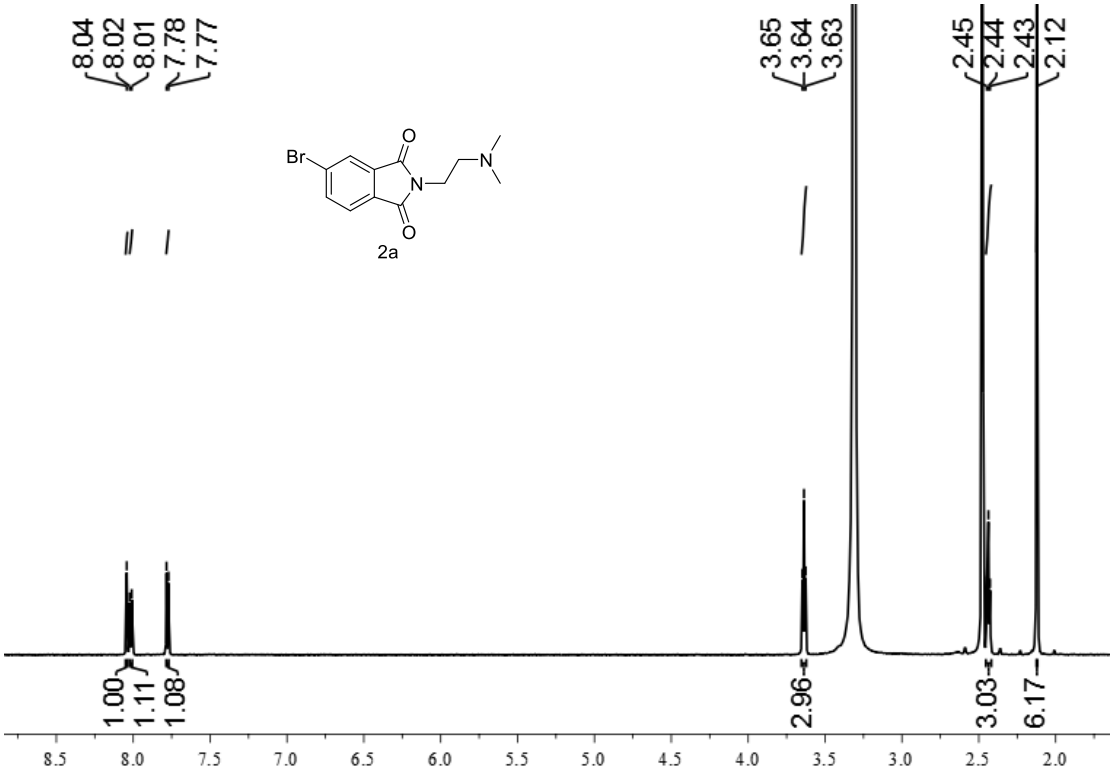

Figure S31. ^{1}H NMR spectra recorded (600 MHz, DMSO, 298K) for compound **2a** (1.0 mM) .

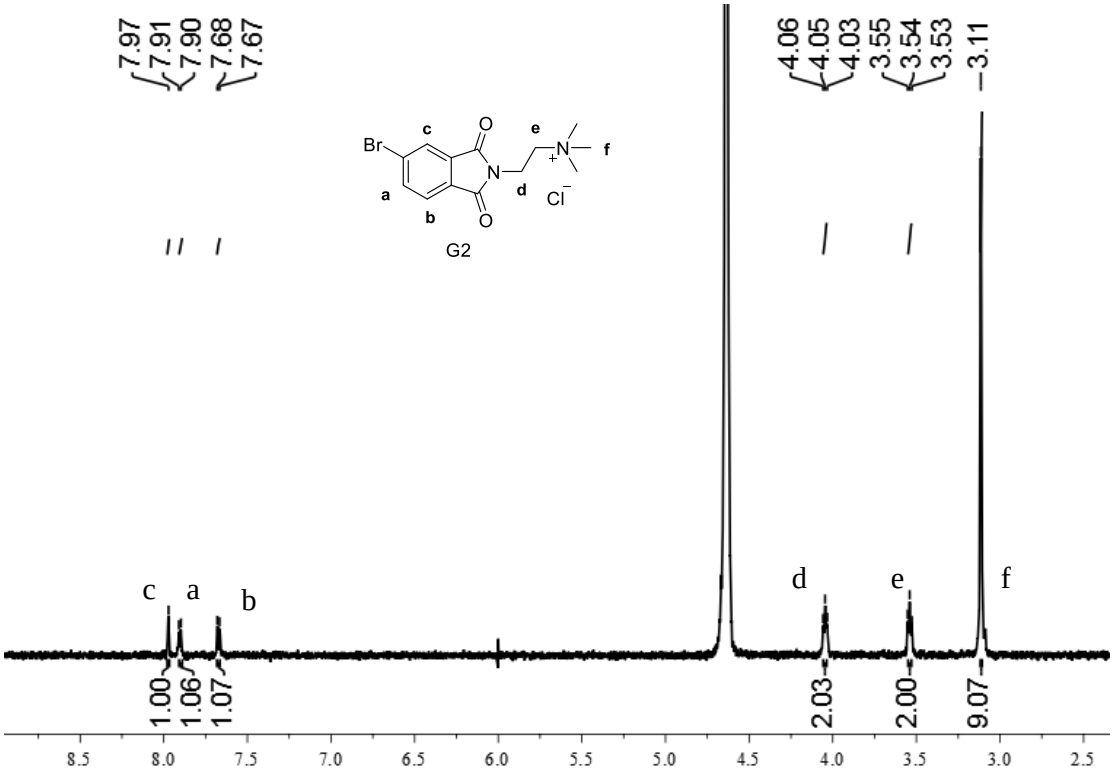

Figure S32. ^{1}H NMR spectra recorded (600 MHz, D_2O, 298K) for compound **G2** (1.0 mM).

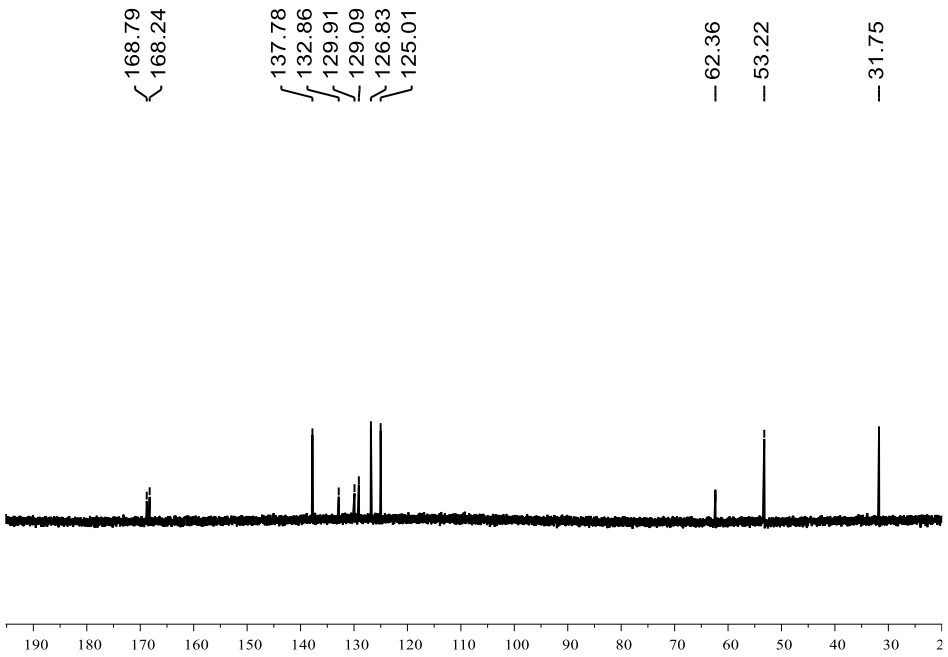

Figure S33. ^{13}C NMR spectra recorded (600 MHz, D_2O, 298K) for compound **G2** .

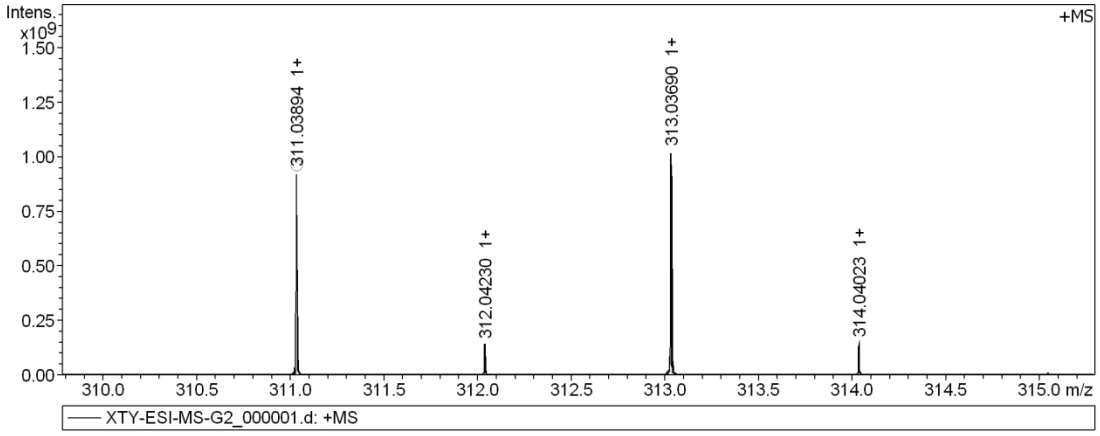

Figure S34. HRMS (ESI) spectrum of **G2**.

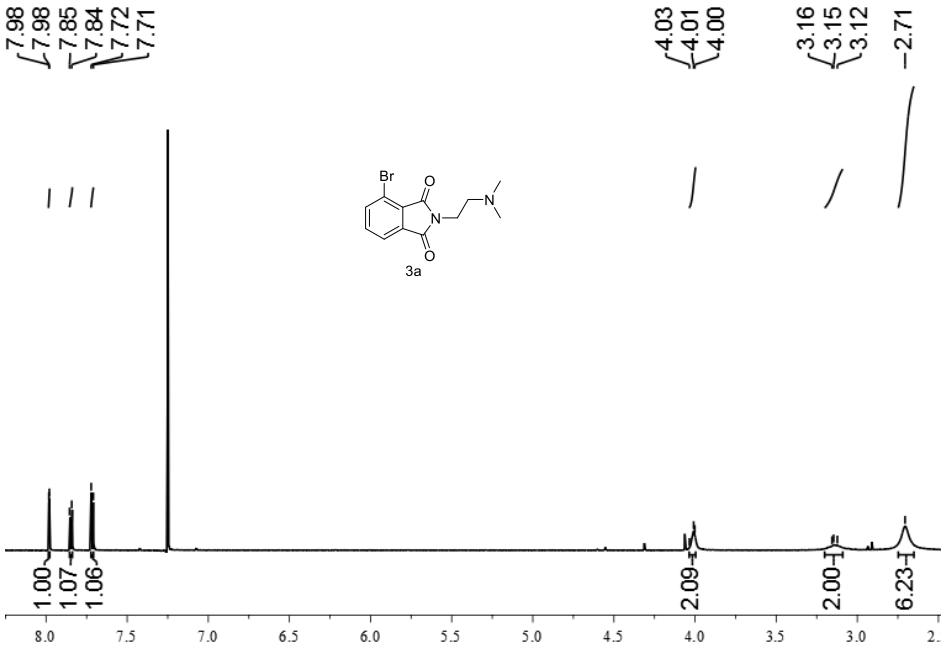

Figure S35. ^{1}H NMR spectra recorded (600 MHz, $CDCl_3$, 298K) for compound **3a** (1.0 mM) .

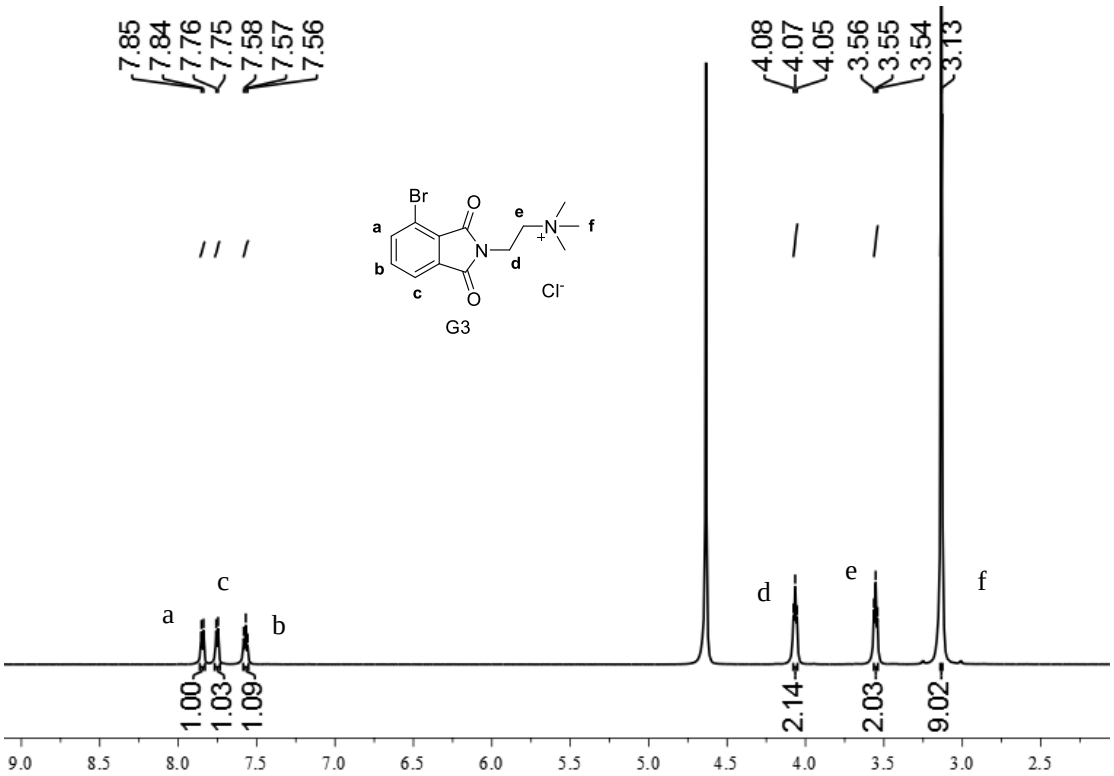

Figure S36. ^{1}H NMR spectra recorded (600 MHz, D_2O, 298K) for compound **G2** (1.0 mM).

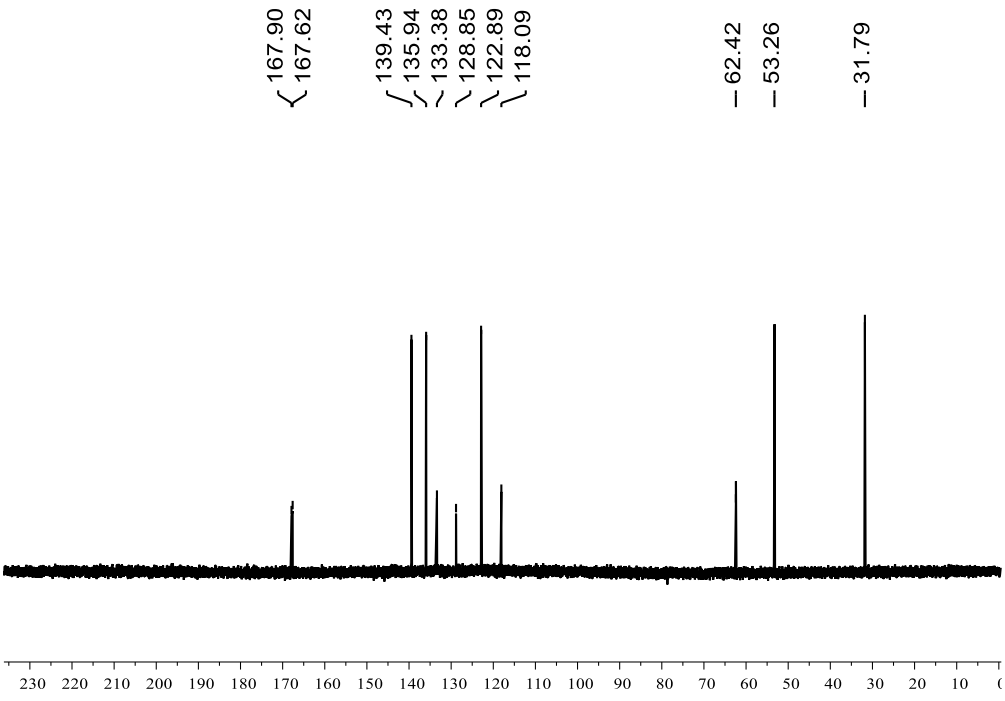

Figure S37. ^{13}C NMR spectra recorded (600 MHz, D_2O, 298K) for compound **G3**.

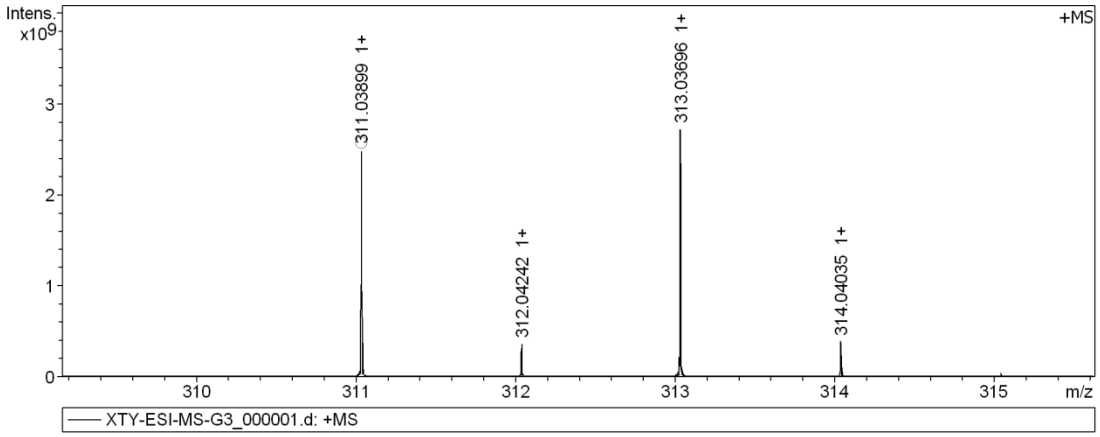

Figure S38. HRMS (ESI) spectrum of **G3**.

Reference

1 Day, A.; Arnold, A.P.; Blanch, R.J.; Snushall, B. Controlling factors in the synthesis of cucurbituril and its homologues. *J. Org. Chem*. **2001**, *66*, 8094–8100.

2 Yang, X.; Zhao, Z.; Zhang, X.; Liu, S. Probing guest compounds enabling the facile isolation of cucurbit[10]uril. *Sci. China. Chem.* **2018**, *61*, 787–791.

3 Guo, X.; Kim, F.S.; Jenekhe, S.A.; Watson, M.D. Phthalimide-based polymers for high performance organic thin-film transistors. *J. Am. Chem. Soc.* **2009**, *131*, 7206-7207.

4 Chen, D.; Zhao, Y.; Zhong, C.; Gao, S.; Yu, G.; Liu, Y.; Qin, J. Effect of polymer chain conformation on field-effect transistor performance: synthesis and properties of two arylene imide based D–A copolymers. *J. Mater. Chem.* **2012**, *22, 14639.*